

Static and Dynamic Behavior of Lens-Type Shear Panel Damper for Highway Bridge Bearing

Tatsumasa Takaku, Feng Chen[†],
Takashi Harada, Masayuki Ishiyama, Nobuhiro Yamazaki^{††},
Tetsuhiko Aoki^{†††}, and Yuhshi Fukumoto^{††††}

Abstract This paper describes a lens-type shear panel damper newly developed for highway bridge bearing. 1),2),3) It utilizes low yield steel LY100 and concave lens shape. Both low yield strength and high ductility are the major requirements for damping devices. Both responses by static and dynamic shear tests result in rectangular shape of load-displacement hysteretic loops with high quality damping. The failure at ultimate state highly depends on the cumulative deformation capacity of panel identity. Damage and life cycles can be estimated by Miner's rule. Prediction matches well with the testing results. Large deformation of steel with high speed strain rate generates a lot of heat leading to high temperature of 300~400 °C at surface. Earthquake energy is converted to both strain and heat energies, which results in large energy dissipation.

1. Introduction

Herein, the results of experimental works are mainly reported even though experimental and analytical works have been investigated in parallel. Static and dynamic tests have been conducted by half size model to examine the fundamental properties of the damper. Thereafter, several seismic excitations of level 2 earthquakes were imposed to the specimen based upon the fundamentals. Random loading tests have been done to evaluate the structural and the functional performances of the damper under design level earthquakes and at the same time to determine the safety margin against collapse under exceeding big earthquakes. For evaluation of fracture, two types of formula, damage index method and damage pass method, are proposed.

2. Damper, Specimen and Test Set-up

2.1 Lens-Type Shear Panel Damper And Half Size Model (Figure-1)

Figure-1 illustrates the panel details of half size model of prototype for test use. Table-1 explains the properties of shear panel. In general, a damper is composed of several components and the failure mechanism is rather complicated. A proposed shear panel has consists of only a single plate element, and failure mode is limited inside of the panel. In order to get a better damping performance, the panel details are modified according to the tests.

2.2 Specimen and Test Set-up (Figure-2, Table-1, Table-2)

Mechanical properties of the panel and the low yield steel of JFE-LY100 are specified in Table-1 and Table-2, both by nominal values. Test set-up is illustrated in Figure-2. Specimen is set to the actuator whose maximum capacity of stroke, velocity, and load are 250mm, 1200mm/s, and 1000KN, respectively. Friction type HTB and a shear key with small clearance of 0.5mm between sole plates, allowing small rotation, are used to connect the lower and upper set-up beams.

† Toko Engineering Consultants, Ltd., Tokyo, Japan.

†† Nippon Chuzo Co., Ltd, Kawasaki, Japan.

††† Aichi Institute of Technology, Toyota, Japan.

†††† Osaka University, Osaka, Japan.

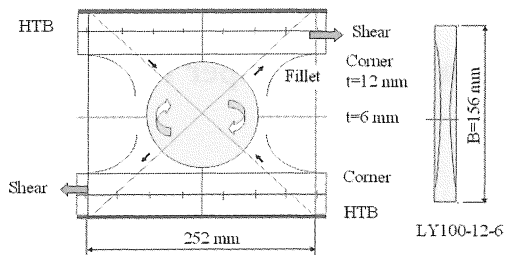


Figure 1: Lens-type shear panel damper:
Panel shape and connection

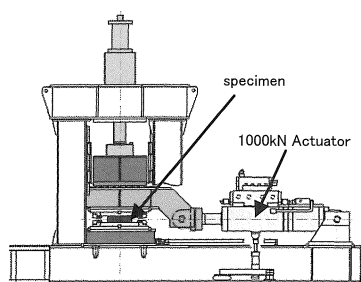


Figure 2: Test set-up

Table-1: Mechanical properties of half size lens panel

LY100-12-6(measured)	
Yield stress(0.2%strain) σ_y	80 N/mm ²
yield displacement(shear strain 3.2%) δ_y	5 mm
yield shear stress $\tau_y = \sigma_y / \sqrt{3}$	46.2 N/mm ²
yield strength Q_y (at lens center, $t=6$ mm)	66.1 KN
yield strength Q_y (at panel edge, $t=12$ mm)	86.5 KN
Max.shear Q_{max} (at base with fillet)	245 KN
Q_{max}/Q_y	2.80~2.87
δ_{max}/δ_y	8~10
δ_{max}	40~50 mm

Table -2: Mechanical properties of low yield steel

(JFE LY100,nominal) , LY100-12-6	
Steel grade	LY-100
Yield strength	80~120 N/mm ²
Tensile strength	200~300 N/mm ²
Yield ratio	<60%
Elongation	>50%
Charpy value (at 0°C)	>27 J
Panel size, B/t	156*156*12mm,13
Concave lens (diameter, t)	130mm, $t=6\sim 12$ mm
Fillet	$R=4t=48$ mm

3. Static and Dynamic Loading Tests

3.1 Static Tests: Gradually Increased Loading ($\Delta Y \sim 10\delta_y$, Shear Strain 3.2%~32%, Table-4)

Cyclic lateral load is applied to the top of set-up beam. The increment of shear displacement in each cycle is $\pm\delta_y$, where $\delta_y=5$ mm is the shear yield displacement corresponding to the

0.2% offset yield shear stress of LY100 (Table-1, Table-2).The displacement cycles are imposed until collapse at the final stage. One cycle is equivalent to shear strain of 3.2%. In the static loading tests, $10\delta_y$ which is equivalent to the shear strain of 32% are recorded at the final stage, where severe cracking damage with large out-of plane twisted deformation is observed. That is left as residual deformation.

3.2 Sinusoidal Loading Tests: Harmonic Motion of SIN Wave With Constant Amplitudes

Six kinds of amplitudes (5, 10, 20, 30, 35, 40mm) and four kinds of velocity (slow and time periods of 0.5, 1.0, 2.0 sec) are combined as test parameters. Slow speed is equivalent to static loading.

4. Fundamentals of Lens-Type Shear Panel: Static and Dynamic Test Results

4.1 Lens Behavior-1: Concave Depth and Failure Modes (Figure-3), "Lens Makes up Flexibility"

In general, when flat steel plate increases in thickness, it increases in strength, while decreases in ductility. Lens type shear panel makes the best use of this property by changing lens thickness and controlled failure modes. It is so designed to combine thicker edge and thin concave that allow low strength and high ductility with use of low yield steel LY100. Failure mode highly depends on the concave depth. When concave depth becomes rather deep, failure moves from lens edge and corners to lens center where cross sectional area is smallest in panel. Figure-3 shows static test results of various shapes of lens. In static tests of LY100-12-8, LY100-12-6, and LY100-12-4, the maximum displacements count up to $8\delta_y$, $9\delta_y$, and $10\delta_y$ in proportion to concave deepness. On the contrary, LY100-12-3 reveals different behavior. It collapsed at edge and center at the same time when the maximum displacement is $8\delta_y$. Early crack initiation at lens center due to the alternate tension field was observed. This phenomenon is more clearly observed in dynamic test. Taking safety margin into consideration, LY100-12-6 is recommended to be the best use for shear panel dampers.

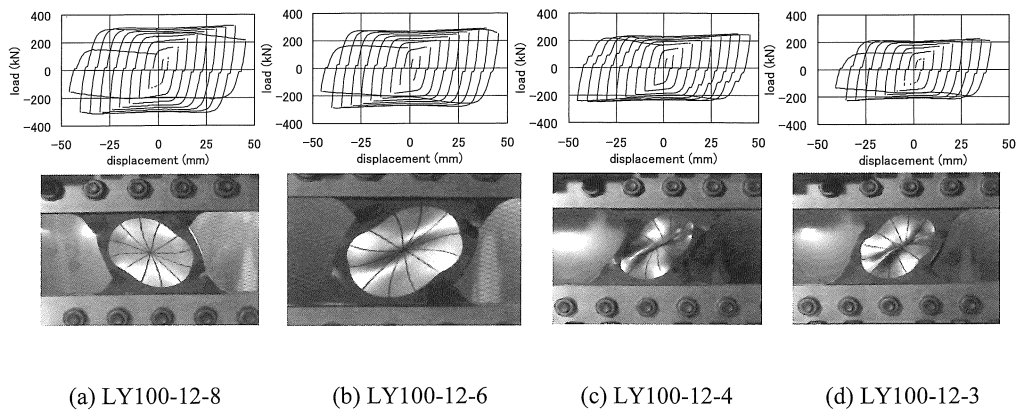


Figure 3: Lens behavior-1: Concave depth and failure modes

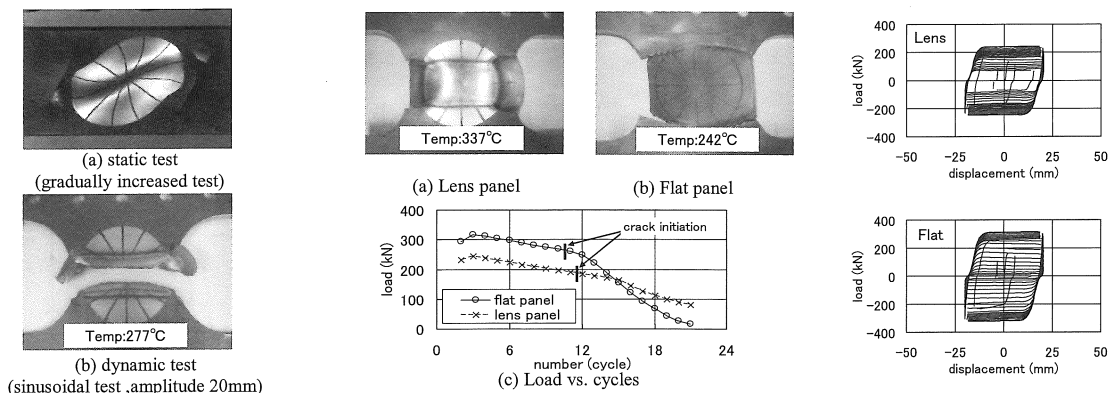


Figure 4: Lens behavior-2: fillet and failure modes ($R=6.5t=78\text{mm}$)

Figure 5: Lens behavior-3: lens panel and flat panel, load versus loading cycles (Sinusoidal test, amplitude 20mm, $T=1\text{sec}$)

4.2 Lens Behavior-2: Fillet and Failure Modes (Figure-4),
 "Too Large Fillet Cut Lens Center"

Panel corner fillet plays an important role to reduce local stress concentration and consequently, to control failure mode of cracking. When fillet is too large in size, cracking initiates at the lens center. In design sense, it is preferable to fail at the four corners instead of lens center for better ductility. Figure-4 shows the $R=6.5t$ case. In static tests, peak shear of $R=4t$ and $R=6.5t$ are 291kN and 330kN, respectively where cracks initiate at the same panel corners. In dynamic test, both cases show different types of failure modes. In the case of $R=4t$, cracks stay at corners. While for $R=6.5t$, cracks initiate at center. In the case of $R=4t$ (Figure-5(a)), wider plastic zone and higher temperature up(377°C) are recognized than that of $R=6.5t$, which imply that the panel with $R=4t$ has better ductility.

4.3 Lens Behavior-3: Lens Panel and Flat Panel (Figure-5),
 "Flat Panel Is Fragile in Dynamics"

Figure-5 shows the dynamic test results; failure modes of

LY100-12-6 (lens) and LY100-12-12 (flat) for constant amplitude of $\pm 20\text{mm}$. In static test, they show the similar failure mode. In proportion to the cross sectional area, the shear force is recorded to be 245kN and 315kN, respectively. In contrast to static test, the dynamic test results provide different type of behavior definitely. In the case of LY100-12-6, plastic zones accompanied with heat radiation spread out widely in radial direction from center to outside, with high temperature of 337°C at the surface. In the case of LY100-12-12, the plastic zone is limited to a narrow band with less temperature of 242°C. Figure-5 shows loads versus repeated cycles. After 12 cycles, significant crack damage at the edges by cracks causes sudden drops of deterioration. Passage of crack propagation left irregularity like gear notch.

4.4 Panel Connection: Use Friction Type HTB (Figure-6),
 "Boundary Changes Ductility"

Major requirement for the specimen connections is as follows:

1. It should transfer seismic lateral forces to shear panel damper tightly with strong enough rigidity so that damping effect is performed completely.

2. Panel edges should be so tightly fixed that it resist both against moment and shear. It is recommended to set double array HTB rather than single arrangement. Single array HTB allows slight rotation due to moment, which results in semi-rigid connection.

3. At the ultimate state of failure, the cracking in tension state is more critical than buckling in compression. Friction type HTB is available to reduce stress concentration with less local constraints. Large deformation causes big thickness change in 3-dimensional direction so that it results in cracking at constraint points such as welding deposits.

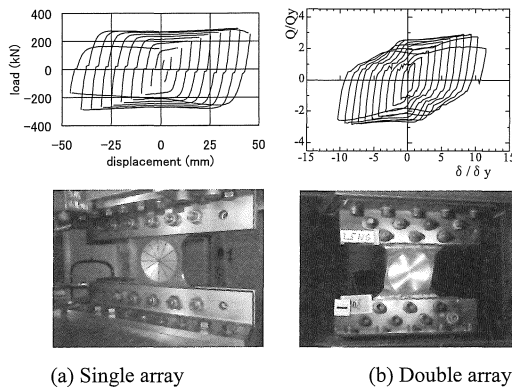


Figure 6: Panel connection: Use HTB (friction type)

Figure-6 shows the panel behavior connected by single (Case A) and double (Case B) array HTB. In Case A and B, $Q_{max}/Q_y=2.8\sim 2.87$, $2.8\sim 2.90$, and $\delta_{max}/\delta_y=9, 10$, respectively. Note that the boundary changes both strength and ductility. Since size of specimen is limited to small one by loading frame and actuator, half size model with single array HTB are planned in this project (Case B was tested in AIT).

4.5 Analytical Model: Bilinear Model With Rectangular Shape by Static and Dynamic Tests (Figure-7)

Figure-7 shows the typical load-displacement hysteric curves for 30mm constant amplitude from the sinusoidal tests results (two cases of slow and $T=1sec$). The peak load gradually decreased with cycles and cracking starts at 6 cycles. Figure-7 also shows an assumed analytical model, a bilinear model of rectangular shape, where two parameters of Q_{max} and $S1$ are defined. The maximum loads, Q_{max} and Q_{peak} are determined;

Q_{max} for the analytical model denotes the average value of resistance shears, and Q_{peak} for design use is the highest value among them. Q_{peak}/Q_{max} is about $1.13\sim 1.18$, both in static and dynamic tests. $S1$ is determined from the unloading gradients. The values of Q_{max} , Q_{peak} , Q_{peak}/Q_{max} and $S1$ are determined to be 245K, 282KN, 1.15 and 140KN/mm, respectively.

5. Cumulative Deformation Capacity (CDC) and Heat Transfer

5.1 Sinusoidal Test Results: CDC and Damage Index (Figure-8, Table-3)

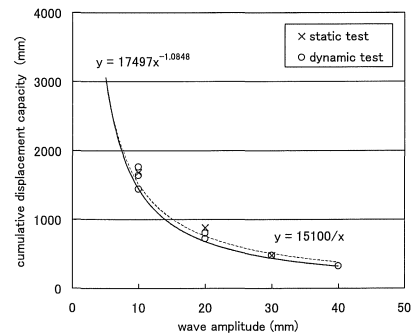


Figure 8: Cumulative displacement capacity versus wave amplitudes

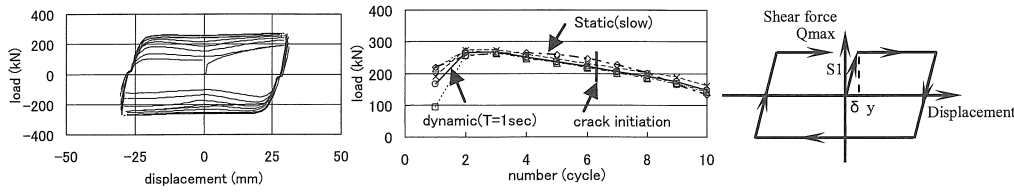
Deformation capacity which is thought to be strain energy capacity, mainly depends on strain rate and magnitude (EQ), stress states and intensity (panel shape) and fracture toughness (LY100). As a performance indicator, cumulative displacement capacity CDC is used for their evaluation. Table-3 summarizes test results (12 cases) which deal with CDC and the number of cycles to failure N_f versus constant wave amplitude x (5, 10, 15, 20, 30, 40 mm). The relationship between cumulative displacement capacity (y , CDC) to the wave amplitude (x) is shown in Figure-8.

$$y = 17497x^{-1.0848} \tag{1}$$

$$xy = 15100 \tag{2}$$

Eq.(1) is derived from test data through regression analysis. Eq.(2) is a simplified hyperbola of Eq.(1) showing $x.y$ is constant which characterizes lens identity. Based on Miner's rule, N_f and damage accumulated in each cycle D_f , are given by Eqs.(3), and (4), respectively.

$$N_f = 15100/4x^2 \tag{3}$$



Sinusoidal test (SIN wave, amplitude 30mm, slow and T=1sec)

 Figure 7: Analytical model: bilinear model with rectangular shape (Q_{max} , S_1)

 Table -3 Sinusoidal test results and cumulative deformation capacity ,damage index $1/N_f$

amplitude x(mm)	period T(sec)	velocity v (mm/s)	num.of cycles to failure Cf	modified cf* d/4x	limit disp. (test results) d(mm)	deformed capacity x*d(mm ²)	critical disp. (Cdc) y=15100/x	num.of cycles to failure Nf=15100/4x ²	damage index 1/Nf
5	1	31	170	168	3360	16800	3020	151	0.0066
10	2	31	38	36	1440	14400	1510	37.8	0.0265
10	1	63	46	44	1760	17600	1510	37.8	0.0265
10	0.5	126	43	41	1640	16400	1510	37.8	0.0265
15	1	94	17	15	900	13500	1007	16.8	0.0596
20	2	63	12	10	800	16000	755	9.4	0.1060
20	1	126	12	10	800	16000	755	9.4	0.1060
20	0.5	251	11	9	720	14400	755	9.4	0.1060
30	2	94	6	4	480	14400	503	4.2	0.2384
30	1	188	6	4	480	14400	503	4.2	0.2384
30	0.5	377	6	4	480	14400	503	4.2	0.2384
40	1	251	4	2	320	12800	378	2.4	0.4238
Specified(averaged) values for design									
18.875	1			10.6	800	15100	800	10.6	0.094

Table-4 Gradually increased loading tests: cumulative deformation and design limit

loading	amplitude	Trav. pass $\Sigma(4x)$	damage index method			$e=x/18.875$	damage pass method		
	x(mm)		Nf=15100/4x ²	1/Nf	D1= $\Sigma(1/Nf)$		e*x	Q= $\Sigma(4e*x)$	D2=Q/800
δy	5	20	151.0	0.007	0.007	0.265	1.32	5.3	0.007
$2\delta y$	10	60	37.8	0.026	0.033	0.530	5.30	26.5	0.033
$3\delta y$	15	120	16.8	0.060	0.093	0.795	11.92	74.2	0.093
$4\delta y$	20	200	9.4	0.106	0.199	1.060	21.19	158.9	0.199
$5\delta y$	25	300	6.0	0.166	0.364	1.325	33.11	291.4	0.364
$6\delta y$	30	420	4.2	0.238	0.603	1.589	47.68	482.1	0.603
$7\delta y$	35	560	3.1	0.325	0.927	1.854	64.90	741.7	0.927
$8\delta y$	40	720	2.4	0.424	1.351	2.119	84.77	1080.8	1.351
$9\delta y$	45	900	1.9	0.536	1.887	2.384	107.28	1509.9	1.887
design limit	35	900			D1<1			800	D2<1

$$D_f = 1/N_f \quad (4)$$

Miner's rule gives the design criterion to failure by Eq.(5).

$$D1 = \sum(1/N_f) < 1 \quad (5)$$

For example, in Table-3, when a damper is subjected to harmonic motion with a specified amplitude $x=18.875$ mm, its survival number of cycles N_f and damage index D_f are 10.6 and 0.094, respectively.

By using the analytical data of traveled pass D_{tp} , the damage pass D_{tp}^* is defined by Eq.(6).

$$D_{tp}^* = \sum(\text{damage pass coefficient } e) * (\text{response amplitude } x) = \sum(4x^2/18.875) \quad (6)$$

where, $e=x/18.875$, $CDC=800$ mm. Safety of D_2 can be evaluated by Eq.(7).

$$D2 = \sum(D_{tp}^*/800) < 1 \quad (7)$$

CDC can be evaluated by two kinds of methods: 1) Damage

index method by Eq. (3), (4), and (5); 2) Damage pass method by Eq.(6) and (7). Both results give the same answer exactly, because they stand on the same base of Eq.(2). Damage index method has an advantage to be able to evaluate damage state without determination of cumulative damage pass limit (CDC). A trial simulation is shown in Table-4.

5.2 Gradually Increased Loading Tests and Evaluation of CDC: Design Criterion (Table-4)

Table-4 shows gradually increased loading test results and evaluation of CDC by damage index method and damage pass method. At $7\delta y$, the cumulative damage $D1=\Sigma(1/N_f)$ becomes 0.927, that is, the $D1$ value is close to 1 indicating almost failure. In the static test, the maximum displacement counts up to $9\delta y$ with traveled pass 900mm. In the dynamic test, the

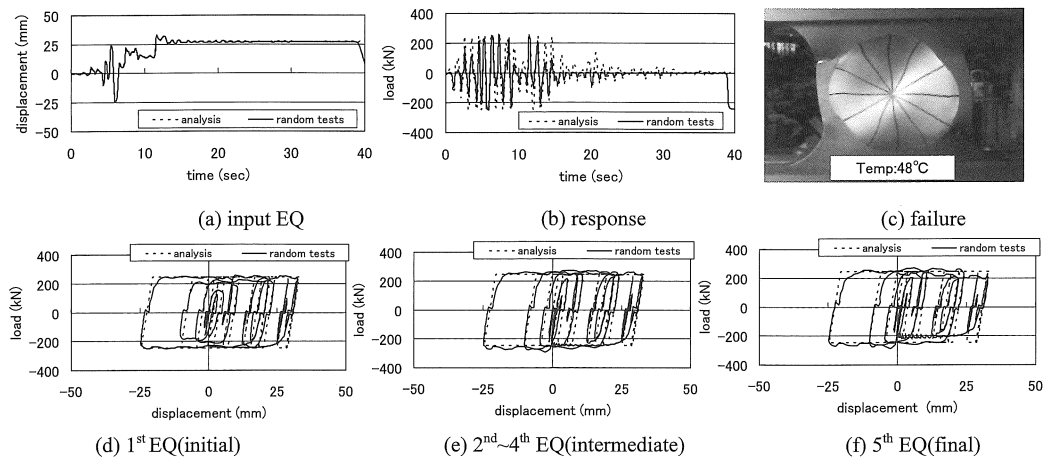


Figure 9: Repeated random loading (level-2,EQ2-2-1,s=1.2) test results:

Time history of displacement and resistance (Q_{peak} , Q_{max})

estimated maximum displacement is reduced to $7\delta_y$, where the damaged traveled pass is 741mm, that is, a little below the cumulative displacement limit value of 800mm. Design criterion can be safely proposed that D_s (static maximum displacement), D_d (dynamic maximum displacement), D_{tp} *(damage pass), can be determined less than 45mm ($9\delta_y$), 35mm ($7\delta_y$), 800mm, respectively.

5.3 Energy Dissipation by Heat Transfer: "High Speed Strain Rate Generates Heat"(Figure-4,5,9)

Large deformation with high speed strain rate generates heat in steel. However, mechanism of heat generation system of steel caused by high strain rate has not been solved yet theoretically in our study. Observations and comments are only described as follows:

1. Heat was generated only in the dynamic test, not in the static test. Slight temperature up was observed in the dynamic random test.
2. Between time period of 0.5 and 2.0 sec., no remarkable difference of heat-up temperature was observed, keeping 300~400°C at the panel surface.
3. Plastic zone and heat radiation spread out widely in the radial direction from lens center to outward.
4. Cracking delay was observed: It seems that expansion due to heat reduces stress concentration. Heat transfer contributes to energy dissipation, consequently good ductility is expected.
5. In random loading, recorded temperature up is limited to 40~50°C, which means that the seismic behavior is close to static one when subjected to actual earthquake.

6. Random Loading and Test Results: Safty Margin and Life Cycle

6.1 Random Loading Tests: Test Planning (EQ, Amplification Factor, Damper Model)

A full scale bridge model and one degree of freedom model with damper are used for dynamic analysis and their responses are provided to the random loading test as displacement control data. Three types of level 2 specified earthquakes (EQ2-2-1, EQ2-2-2, EQ2-2-3)⁴⁾ and their amplification factor (1.0,1.2) are combined. As damper models, stiff (S) and regular(R) models with different stiffness are considered (Table-5).In total, 8 cases (E1~E8) are considered.

6.2 Random Test Results: Comparison With Analysis (Q_{max} , Q_{peak}) (Figure-9, Table-5))

Figure-9 shows test results which explain time history of displacement and shear resistance of damper.

1. Displacement of time history: Loading is applied to the damper by displacement control, therefore input to actuator should be equivalent to output records exactly.
2. Resistance of time history (Q_{max} , Q_{peak}): Damper stiffness model is based upon the hysteretic curves in static tests and analytical model is assumed to be rectangle shape (Figure-7).In half size model, Q_{max} and Q_{peak} is determined to be 245KN and 282KN($Q_{peak}/Q_{max}=1.15$) as damper S-model. Time history of response verifies that damper shear resistance is always within Q_{peak} keeping in safety zones.

Table-5 Random loading test results and comparison with failure prediction

Case	damper model	random loading level-2 EQ	test results: response and cf				prediction by Dtp* and Nf		
			s	cf	max.disp.	travel.pass	Dtp*	800/Dtp*	Nf
E1	R	EQ2-2-1	1	4.5	33.6	325.1	183	4.37	4.37
E2	R	EQ2-2-2	1	5.5	22.9	321.5	160	4.99	4.99
E3	R	EQ2-2-3	1	5.5	14.8	235.3	123.9	6.46	6.46
E4	R	EQ2-2-1	1.2	3	40.3	390.1	263.3	3.04	3.04
E5	R	EQ2-2-2	1.2	4.5	27.5	386	229.3	3.49	3.49
E6	R	EQ2-2-3	1.2	4.5	17.8	265.2	177.1	4.52	4.52
E7	S	EQ2-2-1	1.2	4.5	33.1	332.6	182.9	4.37	4.37
E8	S	EQ2-2-1	1	6	27.6	272.6	124.8	6.41	6.41
estimate1	S	EQ2-2-1	1.2		33.1	327.1	179.7	4.45	4.45
estimate2	S	EQ2-2-1	1.46		40.3	398.0	266.0	3.01	3.01

damper model: R(regular)model;Qmax=225KN,S1=134KN/mm,S(stiff)model ; Qmax=245KN,S1=140KN/mm,Dtp*:damage pass
s:amplification factor, estimate: scaled by a parameter (s) on the basis of E8(s=1)

6.3 Random Test Results: Strength (Safety Margin) and Endurance (Life Cycle)

Table-5 shows endurance test results by repeated random loading. 8 cases of combination with level2 EQ (EQ2-2-1, EQ2-2-2, EQ2-2-3) and amplification factor (1.0, 1.2) are described. For each case, tests results and prediction data are compared with each other. In test, maximum /minimum displacement and number of cycles to failure (c1,c2) are counted. Where c1, c2 are the observed cycles when crack initiation starts and when it reaches to collapse at final state. Average (life) cycle $cf=(c1+c2)/2$ is used for comparison with prediction data. As prediction data, damage index method and damage pass method are used in parallel. Test data of life cycle cf matches well with prediction value Nf within small extent of deviation. As design criterion, it is proposed that Nf is greater than 3, which means that damper should survives at least in three times of level 2 earthquakes. In fact, big earthquakes always accompany middle class earthquakes in sequence at the same site in a few days, without loss time of fixing. It requires that at least Nf should be greater than 2 with much enough safety margin. Shear panel connected by HTB is so designed as to repair easily in a short time once damages are found.

6.4 Influence of Amplification Factor S to Dynamic Response: Dtp* And Nf Are Scaled By s²

Displacements and traveled pass are simply scaled by s. On the other hand, damage pass Dtp* and Nf are scaled by s². Table-5 shows the estimated response values .Nf is easily estimated by the parameter s.

7. Conclusions

1. Shear panel damper is developed as a part of function-separated bearing system to serve for lateral seismic

loads, and it provides easy maintenance and urgent repair works once being damaged.

2. As shear panel damper, concave lens shape +low yield steel LY100 give most effective way to satisfy low strength and high ductility with large energy dissipation.

3. Large deformation of steel with high speed strain rate provides new findings in this research: two items are crucial:1) cumulative deformation capacity, 2)energy dissipation by heat transfer. Both are of great importance to be investigated in the future.

References

[1] Aoki,T.,Liu,Y.,Takaku,T.,Uenoya,M.,&Fukumoto,Y.,200 7.Experimental investigation of tapered shear type seismic devices for bridge bearings.Proc.,8th Pacific Structural Steel Conference (PSSC),New Zealand, March 2007.1,111-117.
 [2] Aoki,T., Liu,Y.,Takaku,T.,&Fukumoto,Y.2008.A new type of shear panel dampers for highway bridge bearings. EUROSTEEL2008,3-5, September 2008,Graz, Austria.
 [3] Aoki,T.,Dang,J.,Zhang,C.,Takaku,T.,&Fukumoto,Y., Dynamic shear tests of low-yield steel panel dampers for bridge bearing. Proc., of 6thInternational Conference of STESSA 2009,16-20 August 2009,Philadelphia, USA.
 [4] Japan Road Association: Specification for Highway Bridges, Part 5, Seismic Design 2000.